OKÜ Fen Bilimleri Enstitüsü Dergisi
5(Özel Sayı):117-134, 2022

OKU Journal of The Institute of Science and Technology, 5(Special Issue):117-134, 2022

Osmaniye Korkut Ata Üniversitesi Fen Bilimleri Enstitüsü Dergisi

Osmaniye Korkut Ata University Journal of Natural and Applied Sciences

Effects of Stacking Sequence on the Structural Performance of Composite Overwrapped Pressure Vessels with Aluminium Liner

Taner COŞKUN[1*], Ömer Sinan ŞAHİN[2]

[1]Konya Technical University, Faculty of Engineering and Natural Science, Department of Mechanical Engineering, 42010, Konya/Turkey
[2]Konya Technical University, Faculty of Engineering and Natural Science, Department of Mechanical Engineering, 42010, Konya/Turkey

[1]https://orcid.org/0000-0002-4815-9278
[2]https://orcid.org/0000-0002-0999-7332
*Corresponding author: tcoskun@ktun.edu.tr

Research Article

Article History:

Received: 15.12.2021
Accepted: 18.01.2022
Published online: 23.02.2022

Keywords:

Dome profile
Filament winding
Geodesic trajectories
Pressure vessels
Stacking sequence

ABSTRACT

Pressure vessels are subjected to stresses in axial and radial directions during their service life, which causes undesirable damages. For that reason, it is highly important to design the fiber directions in composite overwrapped pressure vessels in such a way that can carry the loads occurring in both directions. In this context, composite pressure vessels with 20 mm polar opening radii were designed and composite layers were wound on the aluminium liner with 2 mm thickness. For the aluminium liner, the dome portions were designed with geodesic trajectories and the corresponding profile coordinates were obtained by solving the elliptical integral and using a circular arc. Helical and hoop winding layers were used together on the cylinder surface and the effect of stacking sequence on the structural performance was examined. In the current study, numerical models with six different stacking sequences of hoop winding and helical winding with aluminum liner were defined and thus mechanical properties such as stress, strain and failure indexes were determined. Furthermore, the effects of hoop winding layers utilization on the mechanical properties were investigated by comparing with the numerical model consisting of completely helical winding layers.As a result of the current study, it has been concluded that the hoop winding layers have favorable effects on mechanical properties. It has also been observed that the utilization of the hoop winding layers provides an improvement of approximately 31.42% in the failure index compared to the numerical model consisting of completely helical winding. Additionally, it was observed that although the stacking sequence for the hoop winding was highly effective on the interlaminar shear stress, it did not have much effect on the stress/strain results and the failure indexes.

İstifleme Sırasının Alüminyum Astarlı Kompozit Katmanlı Basınç Kaplarının Yapısal Performansına Etkileri

Araştırma Makalesi

Makale Tarihçesi:

Geliş tarihi: 15.12.2021
Kabul tarihi: 18.01.2022
Online Yayınlanma: 23.02.2022

ÖZET

Basınçlı kaplar hizmet ömürleri boyunca eksenel ve radyal yönlerde gerilmelere maruz kalmakta ve bu durum istenmeyen hasarlara neden olmaktadır. Bu sebepten dolayı kompozit katmanlı basınçlı kaplarda fiber

Anahtar Kelimeler:

Kubbe profili
Filaman sarım
Jeodezik yörünge
Basınç kapları
İstif sırası

yönlerinin her iki yönde oluşan yükleri taşıyabilecek şekilde tasarlanması oldukça önemlidir. Bu kapsamda 20 mm kutup ağzı yarıçapına sahip kompozit basınçlı kaplar tasarlanmış ve 2 mm kalınlığındaki alüminyum astar üzerine kompozit tabakalar sarılmıştır. Alüminyum astar için kubbe kısımları jeodezik yörüngelerle tasarlanmış ve eliptik integral çözülerek ve çember yay kullanılarak ilgili jeodezik profil koordinatları elde edilmiştir. Silindir yüzeyinde helisel ve çember sargı tabakaları bir arada kullanılmış ve istifleme sırasının yapısal performansa etkileri incelenmiştir. Bu çalışmada alüminyum astarlı altı farklı çember ve helisel sarım istif sırasına sahip sayısal modeller tanımlanmış ve böylece gerilme, gerinim ve hasar indeksleri gibi mekanik özellikler belirlenmiştir. Ayrıca, tamamen helisel sarım katmanlardan oluşan sayısal model ile karşılaştırılarak, çember sarım tabakaların mekanik özellikler üzerindeki etkileri araştırılmıştır. Mevcut çalışma sonucunda, çember sarım tabakaların mekanik özellikler üzerinde olumlu etkileri olduğu sonucuna varılmıştır. Ayrıca çember sarım tabaka kullanımının tamamen helisel sarımdan oluşan sayısal modele kıyasla hasar indeksinde yaklaşık %31.42 iyileşme sağladığı gözlemlenmiştir. Ek olarak, çember sarım tabakalar için istifleme sırasının katmanlar arası kayma gerilmesi üzerinde oldukça etkili olduğu fakat gerilme/gerinim sonuçları ile hasar indeksleri üzerinde çok fazla etkisi olmadığı gözlemlenmiştir.

To Cite: Coşkun T., Şahin ÖS. Effects of Stacking Sequence on the Structural Performance of Composite Overwrapped Pressure Vessels with Aluminium Liner. Osmaniye Korkut Ata Üniversitesi Fen Bilimleri Enstitüsü Dergisi 2022; 5(Özel sayı): 117-134.

Nomenclature

ρ	Density	**z**	Axial Coordinate
E	Young's Modulus	**R**	Cylinder Radius
G	Shear Modulus	$\mathbf{r_0}$	Polar Opening Radius
v	Poisson's Ratio	**α**	Filament Winding Angle
r	Radial Coordinate	$\mathbf{R_0}$	Circle Arc Radius

Introduction

Composite materials have many advantages over conventional materials such as high strength/weight ratio, fatigue and corrosion resistance (Takeichi et al. 2003; Zuttel, 2003). Due to these advantages, the utilization of composite materials in automotive, aviation, wind, petroleum, pressure vessels, medical and sports products is continuously increasing (Elmar and Bernhard, 2015). These materials are subjected to various stress levels in the usage areas and different damage mechanisms occur accordingly. Therefore, many studies have been carried out to determine the mechanical properties of composite materials. Yao et al. (2018) conducted a literature review on advanced surface treatment techniques and the production of carbon fiber reinforced thermoplastic composites. In this study, the advantages and disadvantages of using carbon fiber in thermoplastic composites were also examined and it was stated that carbon fibers have a lower density, higher strength and wear resistance compared to glass fibers. On the other hand, it was stated that unidirectional carbon fibers exhibit lower strain than glass fibers and are more expensive. In another study, Oromiehie et al. (2019) conducted a

literature review on the automated fiber placement method, which is one of the composite production techniques, and examined the effects of defects occurring during the production process on the final properties.

Many studies have been conducted in the literature to determine the mechanical properties of composite pipes. Gemi (2014; 2018) performed static burst and fatigue tests on glass fiber reinforced plastic composite pipes produced with various winding angles. Apart from that, Gemi et al. (2009) investigated the fatigue life of composite pipes with a ±75° winding angle. In the study conducted by Gemi et al. (2020), the mechanical properties and machinability characteristics of carbon and glass fiber reinforced hybrid composite pipes with various stacking sequences were experimentally investigated. In this context, composite pipes were subjected to hardness, ring tensile, burst and machinability tests. It was seen from the results that the stacking sequence was highly effective on the mechanical properties and the thrust force generated during drilling. Furthermore, considering the mechanical and machinability properties, the optimum stacking sequence was determined as glass/carbon/glass. In another study, Tasyurek and Tarakcioglu (2017) investigated the fatigue behavior of glass fiber reinforced composite pipes with a 55° winding angle and experimentally determined the effects of carbon nanotube addition with different mass ratios on the final results. Furthermore, the effects of surface cracks with different aspect ratios were also examined. It was determined that the use of carbon nanotubes improved the interlaminar adhesion quality, and hence the fatigue life of composite pipes. However, it was concluded that the carbon nanotubes ratio was effective on the results, and a significant improvement in the burst strength and fatigue life was achieved with the use of nanotubes at low mass ratios. In the study conducted by Gemi et al. (2021), the effects of low velocity impact on the strength of 54, 72 and 96 mm diameter glass fiber reinforced composite pipes were experimentally investigated. In this context, impacts were applied to the composite pipes at 4 different energy levels, and thus damage mechanisms and low-velocity impact behaviors were examined. As a result of the study, it was concluded that low velocity impact had less effect on strength and delamination became the dominant damage mechanism with increasing composite pipe diameter. Furthermore, it was observed that the damage mechanisms diversified, and the delaminated area increased with the ascending impact velocity. In another study conducted by Gemi et al. (2022), glass fiber reinforced composite pipes with 54, 72 and 96 mm diameters produced by the filament winding method were subjected to compression after impact tests. In this way, the losses in the axial strength of the specimens depending on the impact effect were determined experimentally, and also the damage mechanisms were examined. As a result, it was concluded that there were differences in the compression after impact damage responses for impacted and non-impacted composite pipes. While damage in non-impacted pipes was observed as local buckling in the flange region, it was determined that the delaminated area enlarged for the impacted specimens and resulted in splitting in the fiber direction with the effect of local buckling.

Hocine et al. (2009) carried out experimental and numerical analysis of the hydrogen pressure vessels obtained as a result of winding carbon fibers on an aluminium liner by filament winding method. In the analysis, only the cylindrical region was taken into account, and the effect of the fiber orientations on the structural performances was investigated by using three different filament winding angles. In addition, burst pressures were obtained for the pressure vessels with various winding angles is found based on the Tsai-Wu failure criterion. As a result of the study, the maximum burst pressure has been achieved for the 55-60° winding range. In another study conducted by Sepetcioglu (2021), graphene added basalt/epoxy composite pressure vessels were produced using the filament winding method. Specimens with ±55° fiber orientation were subjected to low-velocity impact tests at 7 different energy levels under 50 bar internal pressure, and thus their dynamic responses were investigated. As a result, an increase in the burst pressure for the pressure vessels has been observed with the contribution of graphene. It was also concluded that the graphene additive reduced the amount of absorbed energy for the pressure vessels. In the study conducted by Nebe et al. (2020), it was investigated experimentally and analytically how the stacking sequence affects the structural deformation, laminate quality and burst pressure in composite pressure vessels. As a consequence of the experimental studies, it was observed that the stacking sequence changed the burst pressure by about 67%.

Park and Sakai (2020) developed a 3D mathematical model that can calculate the stresses occurring in fiber-reinforced composite pressure vessels. They used the Tsai-Wu failure criterion to determine the burst pressure and plies in which the failure occurred. As a result of the optimization studies, it was determined that the stacking sequence has a significant effect on the burst pressure. In another study, Ozbek et al. (2019) subjected composite pipes produced by using glass, basalt, and glass/basalt fibers with different fiber orientations to the compression test and examined the failure modes, energy absorption capacities and crush behaviors. It was determined that the increase in fiber orientations caused deterioration in energy absorption capacity and an improvement in crushing load. Furthermore, it has been observed that the pipes manufactured using glass fiber have the highest energy absorption capacity. Prabhakar et al. (2019) studied the mechanical properties of filament wound composite pipes such as buckling, burst, corrosion and durability. According to the minimum damage mechanisms observed with the burst analysis, it has been stated that a ±55 ° winding angle is the optimum value. It has also been determined within the scope of literary studies that 90% of the pipes are produced using glass fiber.

In this study, numerical models of composite overwrapped pressure vessels with six different stacking sequences were defined and analyses were carried out by using the Ansys ACP module. The geodesic dome profile was obtained by solving the elliptic integral. The helical winding angles along the dome and cylinder surface were determined and the structural performance of the pressure vessels was investigated. As a result of the analysis, the effects of hoop winding and stacking sequence on the mechanical properties were determined.

Material and Methods

In the current study, numerical analysis of the pressure vessels with 50 mm cylinder radius and 20 mm polar opening radii was performed. In the numerical models, the cylindrical region length was defined as 300 mm and the composite layers were wound on an aluminium liner with a thickness of 2 mm. 12 helical layers were defined along the dome surface. On the other hand, a total of 24 layers of composite layers containing various numbers of helical and hoop windings were defined along the cylinder surface. 150 Bar internal pressure was applied to the numerical models, and thus the mechanical properties of the composite overwrapped pressure vessels were investigated. In the analysis, the material properties were taken from the Ansys Engineering Data Sources. Epoxy E-Glass UD was used as the composite material and Aluminium Alloy was used as the liner material. Composite and liner material properties are shown in Tables 1 and 2, respectively. Furthermore, stress and strain limits for the composite material are shown in Table 3. Boundary conditions were defined considering the application areas as shown in Figure 1. Furthermore, mesh convergence studies were carried out, and the optimum mesh size and method were determined as 2 mm and quadrilaterals, respectively. In this context, 31356 nodes and 31200 quad elements were used in the numerical models.

Table 1. Composite material properties

Materials	**ρ** [kg/m^3]	**E_x** [GPa]	**E_y** [GPa]	**E_z** [GPa]	**ν_{xy}** [-]	**ν_{yz}** [-]	**ν_{xz}** [-]	**G_{xy}** [GPa]	**G_{yz}** [GPa]	**G_{xz}** [GPa]
Epoxy E-Glass UD	2000	45	10	10	0.3	0.4	0.3	5	3.85	5

Table 2. Aluminium liner material properties

Materials	ρ [kg/m^3]	E [GPa]	v [-]	G [GPa]
Aluminium Alloy	2770	71	0.33	2.67

Table 3. Stress and strain limits for composite material

Direction	**Orthotropic Stress Limits [MPa]**	**Orthotropic Strain Limits [mm/mm]**
Tensile X	1100	0.0244
Tensile Y	35	0.0035
Tensile Z	35	0.0035
Compression X	-675	-0.015
Compression Y	-120	-0.012
Compression Z	-120	-0.012
Shear XY	80	0.016
Shear YZ	46.15	0.012
Shear XZ	80	0.016

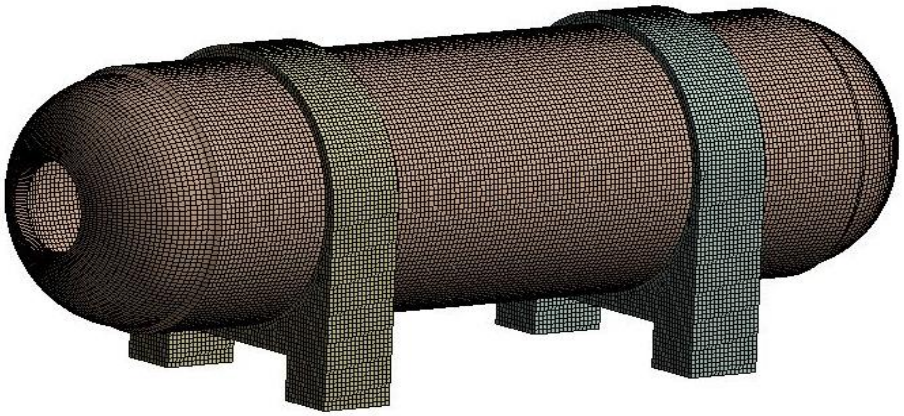

Figure 1. Visualization of the boundary conditions for the composite overwrapped pressure vessels

The geodesic curve represents the shortest distance between two points on any surface. When the composite yarns are wound in the geodesic path, since the fibers follow the stable trajectories, there is no need for friction force to keep the fibers in the defined winding trajectories. In the current study, the geodesic dome profile was obtained in two stages. In the first step, the elliptic integral given in Equation (1) was solved, and thus the axial and radial coordinates from the junction point of the cylinder with the dome to the constant curvature point were obtained (Kabir, 2000; Kumar and Kumari, 2012). The constant curvature point can be expressed as the coordinate at which the elliptic curve has the maximum radius.

$$\bar{z} = -\sqrt{1-\bar{r}_0^2}\int_1^{\bar{r}} \frac{\bar{r}^3}{\sqrt{\bar{r}^2-\bar{r}_0^2-\bar{r}^6(1-\bar{r}_0^2)}}\,dr \qquad (1)$$

Here, $\bar{z}$, $\bar{r}$ and $\bar{r}_0$ denote the dimensionless axial coordinates, radial coordinates and polar opening radii, respectively. As can be seen below, these values are obtained by dividing the axial coordinate, radial coordinate and polar opening radii by the cylinder radius, respectively. Schematic representations of the cylinder radius, polar opening radii, axial coordinates and radial coordinates are demonstrated in Figure 2 on the dome and cylindrical portions.

$$\bar{z} = \frac{z}{R}, \qquad \bar{r} = \frac{r}{R}, \qquad \bar{r}_0 = \frac{r_0}{R}$$

In the second step, a circular arc was used from the constant curvature point to the polar opening, thus completing the dome profile. The circular arc radius is the same as the constant curvature point radius and is obtained (Cai et al., 2019) using Equation (2).

$$R_\theta = \frac{R}{sin2\alpha_0} \qquad (2)$$

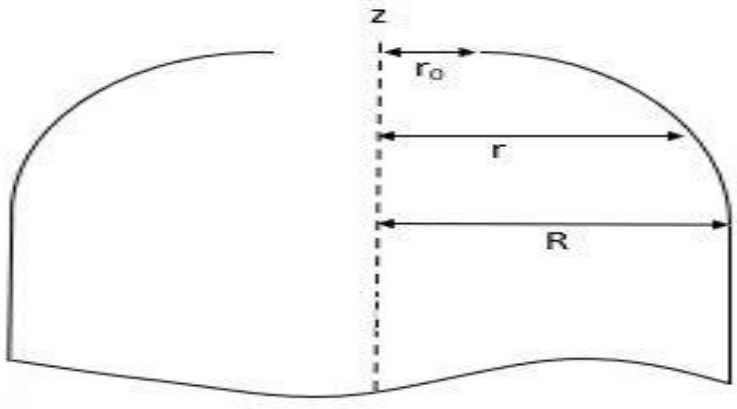

Figure 2. Schematic representation of the dome and cylindrical portions

Depending on the polar opening radii and cylinder radius, only one fiber orientation can be used in the pressure vessels with a geodesic dome profile. Although composite yarns are wound with a defined fiber orientation on the cylindrical surface, this situation is completely different for the dome surface. The filament winding angle is systematically increased up to 90° along the geodesic dome trajectory so that the composite yarns are wound tangentially to the polar opening. The helical winding angles along the cylinder and dome surface were determined (Zwillinger, 1998) using Equation (3). In this study, the helical winding angle of the cylindrical surface was obtained as ±23.58° depending on the polar opening radii and cylinder radius and the same winding angle was defined for all numerical models.

$$\alpha = \arcsin(\frac{r_0}{r}) \quad (3)$$

It is very well known that composite materials exhibit different strengths according to the longitudinal and transverse loading. Therefore, there may be cases where the helical winding is insufficient for the composite pressure vessels and additional hoop winding layers can be necessary to overcome safely the stresses occurring in the radial directions. For that reason, six different numerical models were defined to examine the effect of the stacking sequence and hoop winding layers on the mechanical properties and design more reliable pressure vessels. Six different stacking sequences used in the numerical analysis were demonstrated schematically in Figure 3.

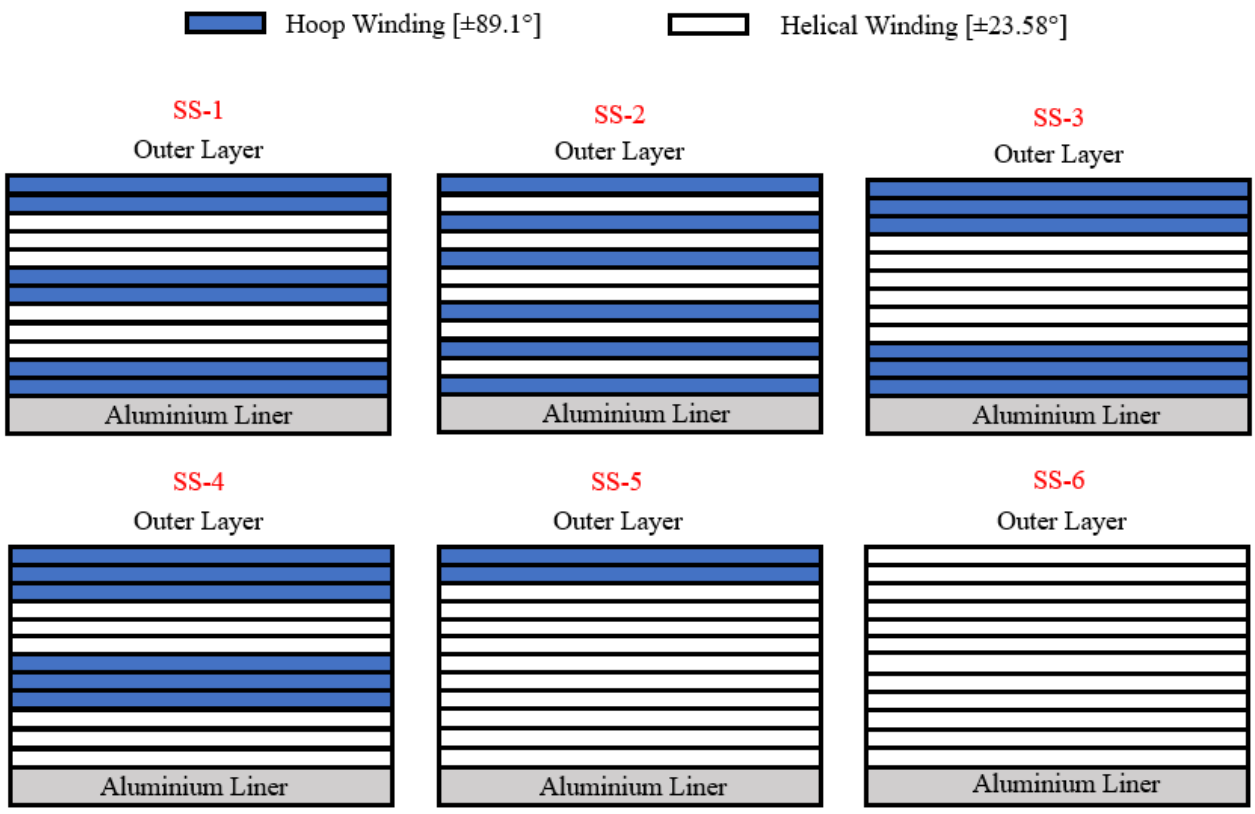

Figure 3. Designations and schematic representation of six different stacking sequences

Results and Discussion

The geodesic dome profile with 20 mm polar opening radii is shown in Figure 4. The dome profile was created using an elliptical curve and a circular arc with a radius of 68.19 mm. Equation 1 was solved by using Matlab subroutine to define the first part of the dome profile and then a circle arc was used to complete the geodesic dome profile shown in Figure 1. On the other hand, the polar opening radii of the pressure vessels must be equal in order to make filament winding in the geodesic trajectories. For that reason, the same profile was used in both dome portions. Apart from that, the filament winding angle along the dome surface is shown in Figure 5. As can be seen from the figure, the fiber orientation at the r = 50 mm, which also represents the winding angle of the cylindrical region, is equal to ±23.58°. In addition, since the composite fibers pass tangentially to the polar opening, the filament winding angle is 90° at the r=20 mm.

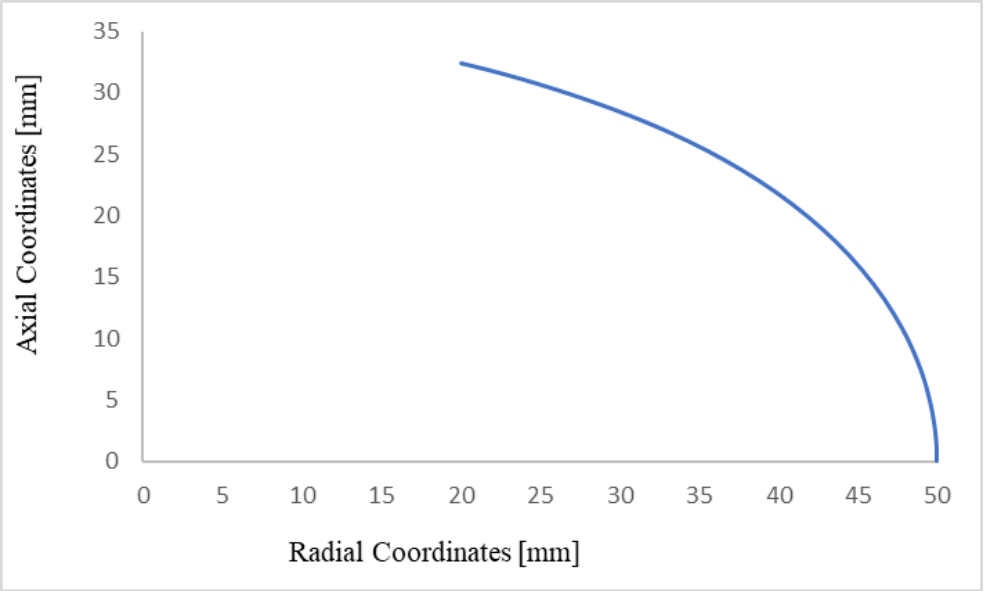

Figure 4. The geodesic dome profile for the pressure vessel with 20 mm polar opening radii

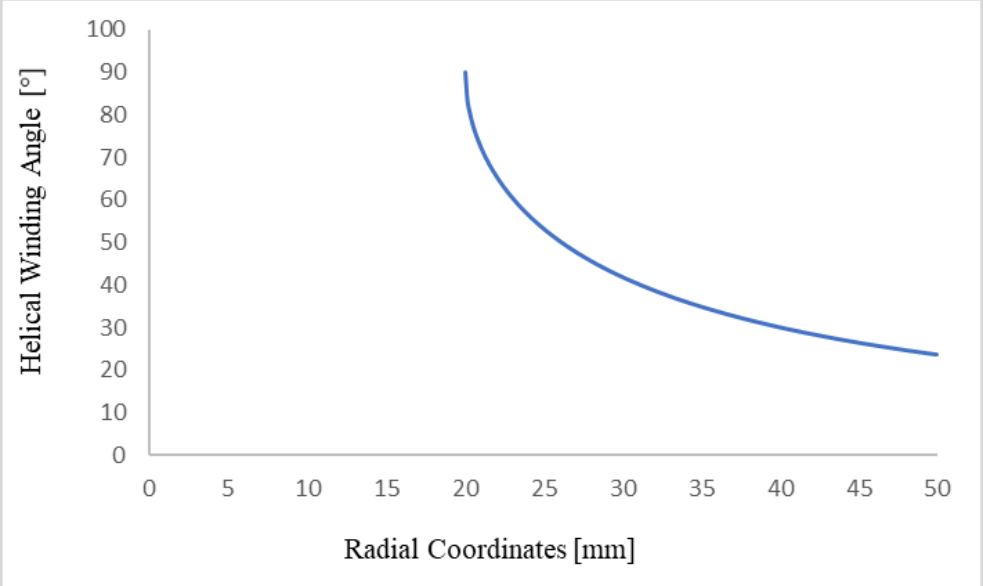

Figure 5. Helical winding angles for the pressure vessel with 20 mm polar opening radii

Since it is not possible to use hoop winding on the dome surface, only 12 helical winding layers are defined in all numerical models. For this reason, the mechanical properties in the dome portions were obtained completely the same for all models. Additionally, since the layers are defined as ±α ° in filament winding, composite layers with +α ° and -α ° fiber orientations generally exhibit the same mechanical properties. Therefore, the transverse and longitudinal stresses were only investigated for the 1st, 3rd, 5th, 7th, 9th and 11th layers in the current study. The maximum longitudinal and transverse stresses occurring on the composite layers from the inner to the outer plies respectively are shown in Figures 6 and 7. It is clearly seen that the lower longitudinal stresses occur in the inner plies and increase continuously towards the outer plies. On the other hand, the filament winding angles changes systematically along the dome surface in composite pressure vessels with a geodesic dome

profile (Butt et al., 2010). Depending on the polar opening and cylinder radii, the composite fibers entering the dome region with a certain winding angle reach 90° towards the polar opening edges. The systematically changing winding angle naturally causes differences in mechanical properties such as transverse/longitudinal stress and strain responses across the dome. This causes various strength properties to be exhibited and the burst pressure to differ in the dome parts (Madhavi, 2009). When Figure 6 is examined, it is seen that the maximum longitudinal stresses take place at the transition point of the dome and the cylinder, and there is a systematic reduction in the stresses towards the polar opening edges. This is an expected result and was completely attributed to the systematic increment of the filament winding angle towards the polar opening and the reduction in the axial stresses carried by the fibers. For instance, the longitudinal stresses were observed as 46.536 MPa in the cylinder-dome transition points for the SS-6 model, while it was determined as 0.38 MPa in the polar opening. Thus, significant changes took place in the longitudinal stresses for the dome parts depending on the winding angle variations. On the other hand, when Figure 7 is examined, it is seen that the transverse stresses are higher around the polar opening edges. This is because the winding angle is around 90° in the polar openings and the radial forces are carried by the fibers. Furthermore, it was observed that the transverse shear stresses decreased from the inner to outer layers. While the maximum transverse stress was obtained as 184.91 MPa in the 1st layer, it was determined as 170.3 MPa in the 11th layer.

Apart from that, longitudinal and transverse stresses for the composite overwrapped pressure vessels are shown in Figure 8. It is clearly seen that there was a decrement in longitudinal and an increment in transverse stresses with the utilization of hoop winding layers. The maximum longitudinal stresses were obtained as 122.46 and 131.92 MPa for the SS-1 and SS-6 stacking sequences, respectively. Thus, approximately 7.73% increment took place in the longitudinal stresses with the utilization of the hoop winding layers. Moreover, the maximum transverse stresses were obtained as 338.33 and 335.93 MPa for the SS-1 and SS-6 models, respectively. It was concluded from the results that the maximum stresses occur in the dome parts and therefore they are the most critical parts of the pressure vessels.

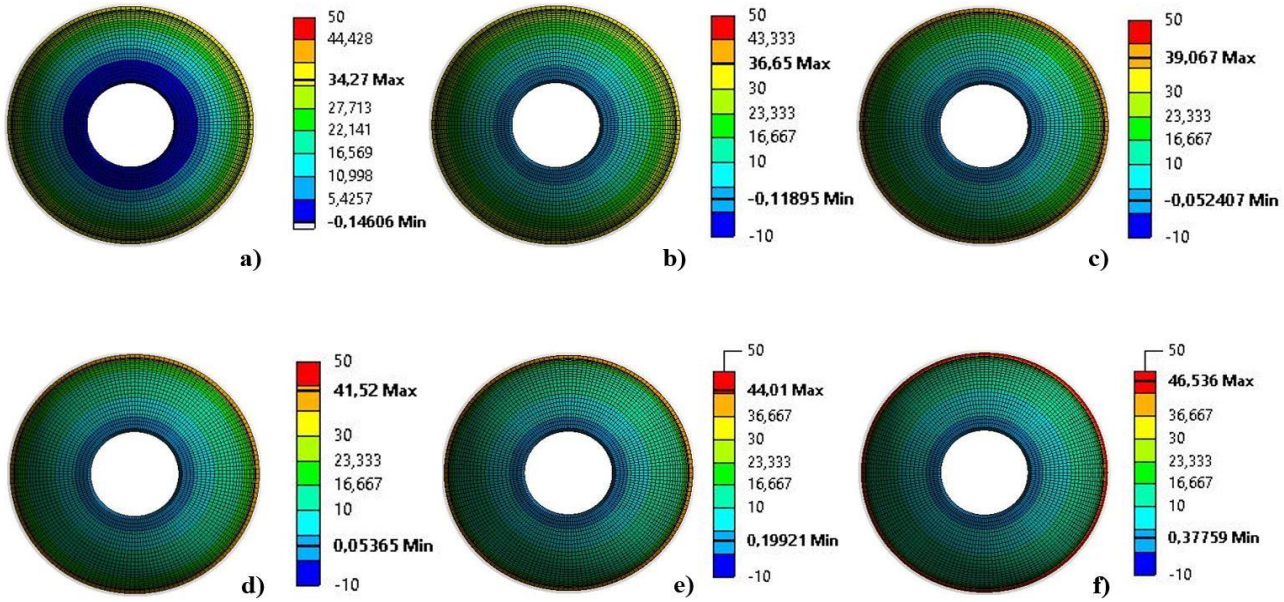

Figure 6. Maximum longitudinal stresses of the dome portions for a) 1st ply, b) 3rd ply, c) 5th ply, d) 7th ply, e) 9th ply and f) 11th ply

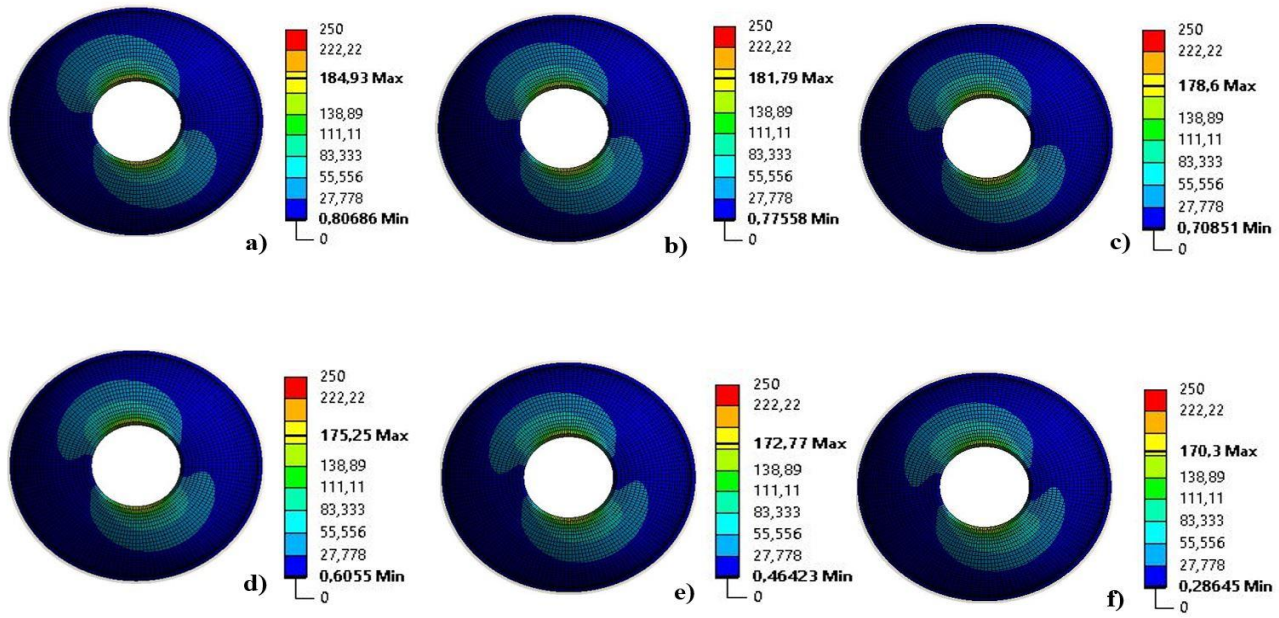

Figure 7. Maximum transverse stresses of the dome portions for a) 1st ply, b) 3rd ply, c) 5th ply, d) 7th ply, e) 9th ply and f) 11th ply

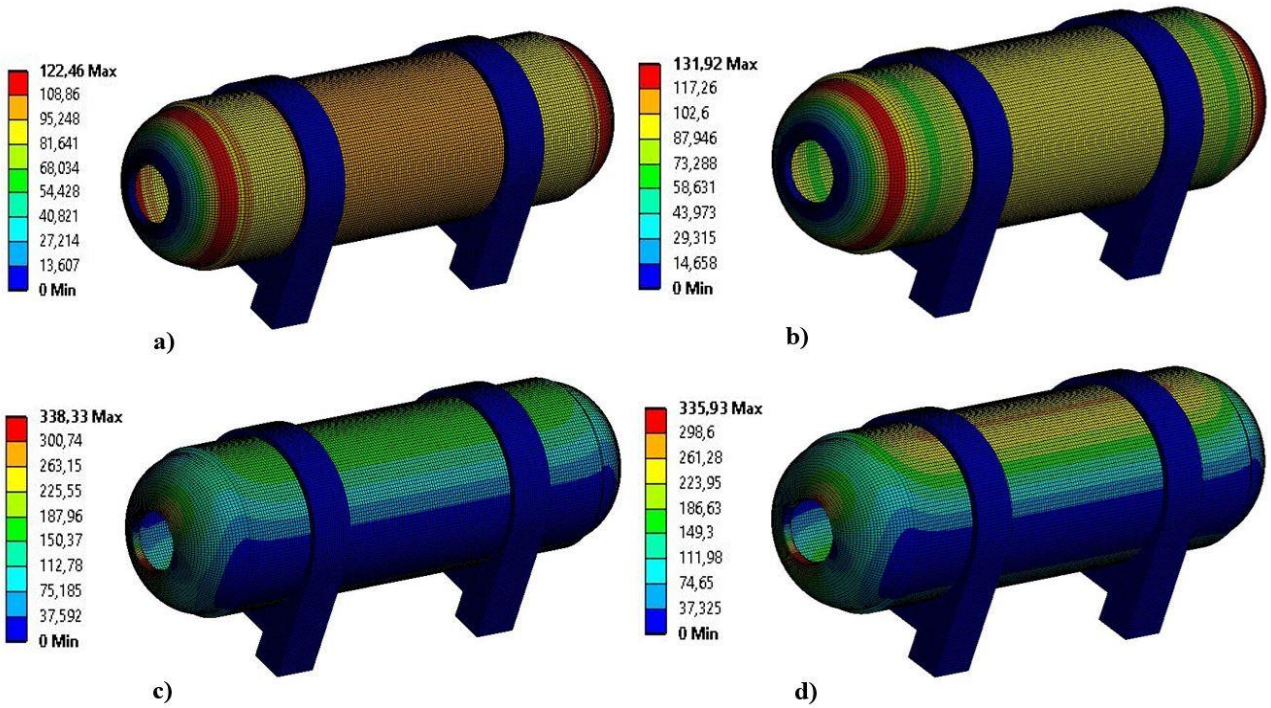

Figure 8. Maximum longitudinal stresses for a) SS-1, b) SS-6 and transverse stresses for c) SS-1, d) SS-6

The increase in the interlaminar shear stress is generally undesirable for the composite materials and leads to various damage mechanisms such as delamination. Therefore, the effects of stacking sequence on the interlaminar shear stresses were examined within the scope of the current study and it was aimed to reduce shear stresses take place in the composite pressure vessels. Interlaminar shear stresses for the numerical models with various stacking sequences are shown in Table 4. As can be clearly seen from the results, the utilization of hoop winding has a reasonably positive effect on the interlaminar shear stresses. For the SS-6 model which completely consists of helical layers, average interlaminar shear stress was obtained as 8.572 MPa. On the other hand, it was determined as 6.6 MPa for the SS-4 model. Thus, approximately 23.01% improvement was achieved in the interlaminar shear stress with the utilization of 12 hoop winding layers. On the other hand, it was concluded that the stacking sequence was not highly effective on the interlaminar shear stress. Among the models with the 12 hoop winding layers, the maximum average interlaminar shear stress was observed in the SS-2 model as 6.927 MPa while the minimum average interlaminar shear stress was observed in the SS-4 model as 6.6 MPa. Therefore approximately 4.72% reduction was achieved by varying stacking sequences. It has also been determined that the critical shear stresses on the structure can be reduced thanks to the use of hoop winding when the favorable effects are considered. Moreover, it has been determined that pressure vessels can be strengthened by optimizing the stacking sequences.

Table 4. Interlaminar shear stress for the composite layers with various stacking sequences

Plies	Interlaminar Shear Stress [MPa]					
	SS-1	**SS-2**	**SS-3**	**SS-4**	**SS-5**	**SS-6**
1-2	6.327	6.202	6.601	10.047	10.180	10.468
2-3	6.362	6.237	6.639	10.003	10.181	10.500
3-4	6.385	10.310	6.665	9.933	10.146	10.498
4-5	6.394	10.191	6.676	9.835	10.078	10.464
5-6	10.168	6.206	6.674	9.711	9.971	10.394
6-7	9.994	6.189	6.658	9.559	9.826	10.289
7-8	9.792	9.790	10.075	5.648	9.643	10.149
8-9	9.564	9.567	9.829	5.591	9.421	9.971
9-10	9.309	5.777	9.554	5.520	9.160	9.756
10-11	9.031	5.708	9.252	5.436	8.861	9.502
11-12	5.224	9.001	8.922	5.339	8.524	9.211
12-13	5.128	8.680	8.566	5.228	8.148	8.882
13-14	5.018	8.337	8.187	8.562	7.735	8.515
14-15	4.896	8.127	8.166	8.563	7.289	8.111
15-16	8.239	4.036	8.269	8.687	6.809	7.669
16-17	8.339	3.889	8.372	8.812	6.808	7.189
17-18	8.438	8.421	8.475	8.936	6.972	6.676
18-19	8.538	8.519	8.577	9.060	7.135	6.128
19-20	8.637	2.526	1.569	1.578	7.299	6.219
20-21	8.737	2.327	1.497	1.416	7.462	6.389
21-22	1.521	8.813	1.515	1.430	2.153	6.558
22-23	1.541	8.912	1.534	1.447	2.178	6.728
23-24	1.560	1.565	1.552	1.464	2.203	6.899
Average	6.919	6.927	6.688	6.600	7.747	8.572
Maximum	10.168	10.310	10.075	10.047	10.181	10.500

The longitudinal and transverse stress/strain results for the models with various stacking sequences are shown in Table 5. It was observed that there was no significant change in the results for the models with 12 helical and 12 hoop winding layers. Based on this it was concluded that the stacking sequence was not highly effective on the longitudinal and transverse stress/strain results. On the other hand, although no significant change in the transverse stress was observed in the SS-5 model, approximately 5.16% increment in the longitudinal stress was took place compared to the SS-1 model. Apart from that, 131.92 MPa longitudinal stress taken place in the SS-6 model which was designed with entirely helical layers and thus approximately 7.73% increase occurred compared to the SS-1 model. These

results show that the number of hoop winding layers is highly significant on the mechanical properties. Additionally, failure indexes for the cylindrical parts of the numerical models were investigated to determine how hoop winding layers affect the mechanical properties, and the results are shown in Figure 9. In the current study, inverse reverse factors which can be defined as an inverse of safety factor were found based on the Tsai-Wu failure criterion. Thus, it was aimed to reduce failure indexes by defining composite layers with various stacking sequences. As can be seen from the figure, similar results were obtained for the SS-1, SS-2, SS-3 and SS-4 models and it demonstrates that the stacking sequence was not significantly effective for the failure behavior. On the other hand, it was seen that this situation was completely different for the SS-5 and SS-6 models, and the decrease in the number of hoop winding layers caused deterioration in the failure indexes. The maximum inverse reverse factor has occurred on the cylinder surface as 0.8065 for the SS-5 model and approximately 25.91% deterioration took place compared to the SS-3 model. Moreover, the inverse reverse factor was obtained as 0.9341 for the SS-6 model and approximately 31.42% improvement was observed compared to the SS-3 model. It was revealed that the SS-6 models should be strengthened under internal pressures above 150 Bar.

Table 5. Longitudinal and transverse stress/strain results for various pressure vessels

	$\sigma_{L,max}$ [MPa]	$\sigma_{T,max}$ [MPa]	$\varepsilon_{L,max}$ [-]	$\varepsilon_{T,max}$ [-]
SS-1	122.46	338.33	0.0010784	0.0047274
SS-2	122.49	338.32	0.0010784	0.0047273
SS-3	122.41	338.35	0.0010785	0.0047277
SS-4	123.85	338.42	0.0011076	0.0047288
SS-5	128.78	336.97	0.0011082	0.0047085
SS-6	131.92	335.93	0.0011093	0.0046938

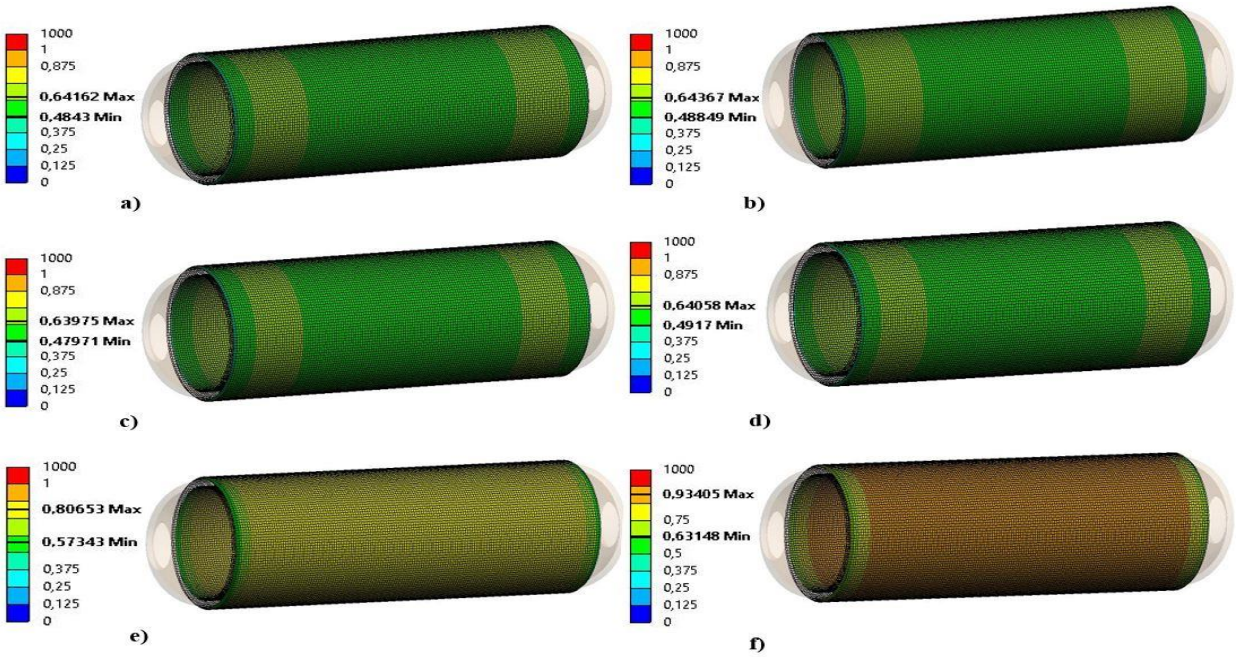

Figure 9. Inverse reverse factors of pressure vessels with various stacking sequences for a) SS-1, b) SS-2, c) SS-3, d) SS-4, e) SS-5 and f) SS-6

Conclusion

In the present study, the effects of the hoop winding layer and the stacking sequence on the strength of the composite overwrapped pressure vessels were investigated. In this context, six numerical models with different stacking sequences of the hoop and helical winding with liner were generated and numerical analyses were carried out with the help of the Ansys ACP module. In the numerical models, aluminium liners with geodesic dome profiles have been designed and then composite layers were defined on the liner surfaces. The stress/strain results for the dome and cylindrical portions were obtained and also the failure behaviors for the six numerical models were investigated. The outcomes achieved from the current study are as follows:

- It has been revealed that the utilization of hoop winding layers is highly effective on the interlaminar shear stresses and reduces the shear stresses. This is because shear stresses are maximum at ±45° and around fiber orientations, and thus the ±23.58° helical winding angles cause higher interlaminar shear stresses than the hoop winding layers. It has also been found that stacking sequences can be optimized to minimize the interlaminar shear stresses since higher shear stresses occur in the inner and outer laminates due to the bending effect.
- It is very well known that the only helical winding layers may be insufficient to meet the radial loads. Therefore, hoop winding layers have been used to strengthen composite pressure vessels against radial loads. As a result, it has been concluded that radial loads are safely carried by the hoop winding laminates, and significant improvement for the failure indexes has been achieved. In this way, maximum inverse reverse factors were obtained as 0.9341 and 0.6398 for the SS-6 and SS-3, respectively, and thus approximately 31.42% improvement in failure indexes has been achieved thanks to the 12 layers of hoop winding.

- From the current study, it was concluded that the dome profile is highly influential on the filament winding angles, and thus the mechanical properties of the composite overwrapped pressure vessels. Since the geodesic dome profile was used in our study, it is not possible to improve fiber orientations to more safely meet the axial and radial loads on the dome portions. Therefore, future studies include using non-geodesic dome trajectories to optimize filament winding angles throughout the dome. Furthermore, the design of hybrid layer overwrapped pressure vessels using carbon and glass fibers can be considered as future works.

Acknowledgement

This work has been performed within the scope of a master's thesis supported by Konya Technical University Graduate School of Natural and Applied Science.

Statement of Conflict of Interest:

Authors have declared no conflict of interest.

Author's Contributions:

The contribution of the authors is equal.

*This study was presented as a summary paper at the International Conference on Engineering, Natural and Applied Sciences (ICENAS'21) held online on 24-26 November 2021.

References

Butt AM., ul Haq SW. Comparative study for the design of optimal composite pressure vessels. Key Engineering Materials 2010; 442: 381-388.

Cai Q., Pu X., Dan L., Li X. Comparative study on multi-type domes of filament-wound composite pressure vessels. In IOP Conference Series: Materials Science and Engineering 2019; 677(2): 022062.

Elmar W., Bernhard J. Composites market report 2014.

Gemi DS., Sahin OS., Gemi L. Experimental investigation of the effect of diameter upon low velocity impact response of glass fiber reinforced composite pipes. Composite Structures 2021; 275: 114428.

Gemi DS., Sahin OS., Gemi L. Experimental investigation of axial compression behavior after low velocity impact of glass fiber reinforced filament wound pipes with different diameter. Composite Structures 2022; 280: 114929.

Gemi L. Düşük hızlı darbe hasarlı filaman sarım hibrid boruların iç basınç altında yorulma davranışı. Doktara Tezi, Selçuk Üniversitesi Fen Bilimleri Enstitüsü, Konya 2014.

Gemi L. Investigation of the effect of stacking sequence on low velocity impact response and damage formation in hybrid composite pipes under internal pressure. A comparative study. Composites Part B: Engineering 2018; 153: 217-232.

Gemi L., Koklu U., Yazman S., Morkavuk S. The effects of stacking sequence on drilling machinability of filament wound hybrid composite pipes: Part-1 mechanical characterization and drilling tests. Composites Part B 2020; 186: 107787.

Gemi L., Tarakcioglu N., Akdemir A., Sahin OS. Progressive fatigue failure behavior of glass/epoxy (±75) 2 filament-wound pipes under pure internal pressure. Materials & Design 2009; 30(10): 4293-4298.

Hocine A., Chapelle D., Boubakar ML., Benamar A., Bezazi A. Experimental and analytical investigation of the cylindrical part of a metallic vessel reinforced by filament winding while submitted to internal pressure. International journal of pressure vessels and piping 2009; 86(10): 649-655.

Kabir MZ. Finite element analysis of composite pressure vessels with a load sharing metallic liner. Composite structures 2000; 49(3): 247-255.

Kumar SS., Kumari AS. Design and failure analysis of geodesic dome of a composite pressure vessel. International Journal of Engineering Research and Technology 2012; 1(7): 1-8.

Madhavi M. Design and analysis of filament wound composite pressure vessel with integrated-end domes. Defence Science Journal 2009; 59(1): 73-81.

Nebe M., Asijee TJ., Braun C., van Campen JMJF., Walther F. Experimental and analytical analysis on the stacking sequence of composite pressure vessels. Composite Structures 2020; 247: 112429.

Oromiehie E., Prusty BG., Compston P., Rajan G. Automated fibre placement based composite structures: Review on the defects, impacts and inspections techniques. Composite Structures 2019; 224: 110987.

Ozbek O., Bozkurt OY., Erklig A. An experimental study on intraply fiber hybridization of filament wound composite pipes subjected to quasi-static compression loading. Polymer Testing 2019; 79: 106082.

Park YH., Sakai J. Optimum design of composite pressure vessel structure based on 3-dimensional failure criteria. International Journal of Material Forming 2020; 13(6): 957-965.

Prabhakar MM., Rajini N., Ayrilmis N., Mayandi K., Siengchin S., Senthilkumar K., Karthikeyan S., Ismail SO. An overview of burst, buckling, durability and corrosion analysis of lightweight FRP composite pipes and their applicability. Composite Structures 2019; 230: 111419.

Sepetcioglu H. Experimental study on the effect of graphene nanoplatelets on the low-velocity impact response of prestressed filament wound basalt-based composite pressure vessels. Polymer Composites 2021; 42: 5527-5540.

Takeichi N., Senoh H., Yokota T., Tsuruta H., Hamada K., Takeshita HT., Tanaka H., Kiyobayashi T., Takano T., Kuriyama N. Hybrid hydrogen storage vessel, a novel high-pressure hydrogen storage vessel combined with hydrogen storage material. International Journal of Hydrogen Energy 2003; 28(10): 1121-1129.

Tasyurek M., Tarakcioglu N. Enhanced fatigue behavior under internal pressure of CNT reinforced filament wound cracked pipes. Composites Part B: Engineering 2017; 124: 23-30.

Yao SS., Jin FL., Rhee KY., Hui D., Park SJ. Recent advances in carbon-fiber-reinforced thermoplastic composites: A review. Composites Part B: Engineering 2018; 142: 241-250.

Zuttel A. Materials for hydrogen storage. Materials Today 2003; 6(9): 24-33.

Zwillinger D. Handbook of differential equations. Gulf Professional Publishing 1998; 1.